

## Article

# 1-(Arylsulfonyl-isoindol-2-yl)piperazines as 5-HT<sub>6</sub>R Antagonists: Mechanochemical Synthesis, In Vitro Pharmacological Properties and Glioprotective Activity

Vittorio Canale <sup>1,\*</sup> , Wojciech Trybała <sup>1</sup>, Séverine Chaumont-Dubel <sup>2</sup> , Paulina Koczurkiewicz-Adamczyk <sup>3</sup> , Grzegorz Satała <sup>4</sup>, Ophélie Bento <sup>2,5</sup>, Klaudia Blicharz-Futera <sup>1</sup>, Xavier Bantreil <sup>5,6</sup> , Elżbieta Pękala <sup>3</sup> , Andrzej J. Bojarski <sup>4</sup> , Frédéric Lamaty <sup>5</sup>, Philippe Marin <sup>2</sup>  and Paweł Zajdel <sup>1</sup> 

<sup>1</sup> Department of Organic Chemistry, Faculty of Pharmacy, Jagiellonian University Medical College, 9 Medyczna Street, 30-688 Krakow, Poland

<sup>2</sup> Institut de Génomique Fonctionnelle, Université de Montpellier, CNRS, INSERM, 34094 Montpellier, France

<sup>3</sup> Department of Pharmaceutical Biochemistry, Faculty of Pharmacy, Jagiellonian University Medical College, 9 Medyczna Street, 30-688 Krakow, Poland

<sup>4</sup> Department of Medicinal Chemistry, Maj Institute of Pharmacology, Polish Academy of Sciences, 12 Śmętna Street, 31-343 Krakow, Poland

<sup>5</sup> IBMM, Université de Montpellier, CNRS, ENSCM, 34095 Montpellier, France

<sup>6</sup> Institut Universitaire de France (IUF), 75005 Paris, France

\* Correspondence: vittorio.canale@uj.edu.pl



**Citation:** Canale, V.; Trybała, W.; Chaumont-Dubel, S.; Koczurkiewicz-Adamczyk, P.; Satała, G.; Bento, O.; Blicharz-Futera, K.; Bantreil, X.; Pękala, E.; Bojarski, A.J.; et al. 1-(Arylsulfonyl-isoindol-2-yl)piperazines as 5-HT<sub>6</sub>R Antagonists: Mechanochemical Synthesis, In Vitro Pharmacological Properties and Glioprotective Activity. *Biomolecules* **2023**, *13*, 12. <https://doi.org/10.3390/biom13010012>

Academic Editor: Zhangguo Gao

Received: 28 November 2022

Revised: 15 December 2022

Accepted: 17 December 2022

Published: 21 December 2022



**Copyright:** © 2022 by the authors. Licensee MDPI, Basel, Switzerland. This article is an open access article distributed under the terms and conditions of the Creative Commons Attribution (CC BY) license (<https://creativecommons.org/licenses/by/4.0/>).

**Abstract:** In addition to the canonical Gs adenylyl cyclase pathway, the serotonin type 6 receptor (5-HT<sub>6</sub>R) recruits additional signaling pathways that control cognitive function, brain development, and synaptic plasticity in an agonist-dependent and independent manner. Considering that aberrant constitutive and agonist-induced active states are involved in various pathological mechanisms, the development of biased ligands with different functional profiles at specific 5-HT<sub>6</sub>R-elicited signaling pathways may provide a novel therapeutic perspective in the field of neurodegenerative and psychiatric diseases. Based on the structure of SB-258585, an inverse agonist at 5-HT<sub>6</sub>R-operated Gs and Cdk5 signaling, we designed a series of 1-(arylsulfonyl-isoindol-2-yl)piperazine derivatives and synthesized them using a sustainable mechanochemical method. We identified the safe and metabolically stable biased ligand **3g**, which behaves as a neutral antagonist at the 5-HT<sub>6</sub>R-operated Gs signaling and displays inverse agonist activity at the Cdk5 pathway. Inversion of the sulfonamide bond combined with its incorporation into the isoindoline scaffold switched the functional profile of **3g** at Gs signaling with no impact at the Cdk5 pathway. Compound **3g** reduced the cytotoxicity of 6-OHDA and produced a glioprotective effect against rotenone-induced toxicity in C8-D1A astrocyte cell cultures. In view of these findings, compound **3g** can be considered a promising biased ligand to investigate the role of the 5-HT<sub>6</sub>R-elicited Gs and Cdk5 signaling pathways in neurodegenerative diseases.

**Keywords:** mechanochemical synthesis; 5-HT<sub>6</sub> receptor inverse agonism/neutral antagonism; Gs and Cdk5 signaling pathways; glioprotective properties; rotenone toxicity

## 1. Introduction

The serotonin type 6 receptor (5-HT<sub>6</sub>R) is a Gs-coupled receptor widely expressed in brain regions involved in cognitive functions [1] and has been considered an important target to alleviate cognitive symptoms related to neurodegenerative and psychiatric disorders [2–6]. Several lines of evidence indicate that modulation of cognition by 5-HT<sub>6</sub>R ligands might be independent of its coupling to Gs, suggesting the engagement of alternative signaling mechanisms. Indeed, interactomic studies revealed that the 5-HT<sub>6</sub>R is linked to different GIPs (GPCR interacting proteins) that underlie its modulation of cognitive (mechanistic target of rapamycin (mTOR)) and neuro-developmental (cyclin-dependent

kinase 5 (Cdk5) and G protein-regulated inducer of neurite outgrowth 1 (GPR1N1)) processes [7,8]. Recently, a non-canonical 5-HT<sub>6</sub>R-elicited Gαq/11-RhoA pathway, which modulates nuclear actin and increases histone acetylation and chromatin accessibility, has been identified in hippocampal neurons [9]. An important feature of the 5-HT<sub>6</sub>R is its high level of ligand-independent constitutive activity, which corresponds to the ability of a receptor to be active even in the absence of an agonist [10]. The role of 5-HT<sub>6</sub>R constitutive activity at canonical Gs signaling and non-canonical signaling has been described in various pathophysiological conditions [11–15]. Consistent with those findings, the development of 5-HT<sub>6</sub>R ligands acting as inverse agonists and/or neutral antagonists at the different 5-HT<sub>6</sub>R-operated signaling pathways is of utmost interest to decipher the cellular mechanism(s) under the control of the various 5-HT<sub>6</sub>R signal transduction mechanisms and of constitutive vs. agonist-dependent receptor activation.

Many ligands were evaluated to study the role of 5-HT<sub>6</sub>R, yet the design of 5-HT<sub>6</sub>R-biased ligands remains highly challenging. Using molecular dynamic simulations, we previously reported structural hints responsible for inverse agonism and neutral antagonism at Gs signaling in a group of imidazo[4,5-*b*]- and imidazo[4,5-*c*]pyridines (Figure 1A) [16,17]. A different approach, based on the truncation of the planar 1*H*-pyrrolo[3,2-*c*]quinoline core present in the 5-HT<sub>6</sub>R antagonist (S)-1-[(3-chlorophenyl)sulfonyl]-4-(pyrrolidine-3-yl-amino)-1*H*-pyrrolo[3,2-*c*]quinoline (CPPQ) [18], to the more flexible 2-phenyl-1*H*-pyrrole-3-carboxamide scaffold, shifted the compound activity from neutral antagonism to inverse agonism at receptor-operated Gs and Cdk5 signaling (Figure 1B) [19].

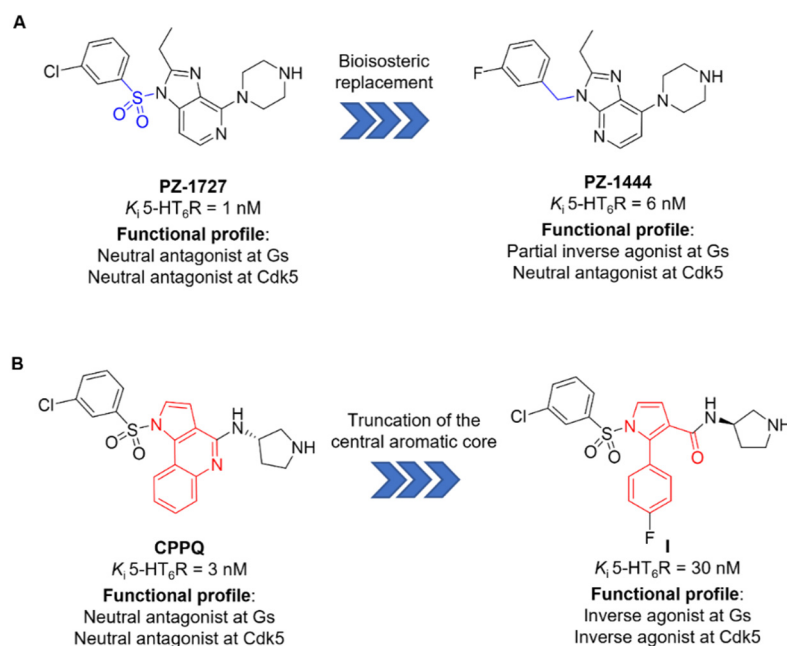


**Figure 1.** Structural determinants responsible for different in vitro activity at 5-HT<sub>6</sub>R-operated Gs and/or Cdk5 signaling pathways in a group of imidazopyridines (A) or pyrroloquinoline/arylpyrrole derivatives (B) [17,19].

These observations prompted us to investigate further the role of the arylsulfonamide fragment in the development of active 5-HT<sub>6</sub>R ligands. Starting from SB-258585, an inverse agonist at 5-HT<sub>6</sub>R-operated Gs and Cdk5 signaling [20,21], we designed a set of 1-(arylsulfonyl-isoindol-2-yl)piperazines. We focused on the inversion of the sulfonamide bond combined with its incorporation into differently substituted isoindoline scaffold and flipping of the piperazine moiety in the 2-, 3-, or 4- position at the phenyl ring (Figure 2).



**Figure 2.** Design of a 1-(arylsulfonyl-isoindol-2-yl)piperazines library.

The impact of compounds synthesized using a mechanochemical approach on 5-HT<sub>6</sub>R-operated Gs and Cdk5 signaling pathways was examined. The glioprotective properties of the selected compound with the highest potency at Gs and Cdk5 signaling and favorable preliminary ADMET profile were investigated in C8-D1A astrocytes exposed to the gliotoxic treatments using 6-hydroxydopamine (6-OHDA) and rotenone (ROT).

## 2. Material and Methods

### 2.1. Chemistry

#### 2.1.1. General Chemical Methods

All commercially available reagents were of the highest purity from Fluorochem, Across Organic. The milling treatments were carried out in a vibratory ball-mill Retsch MM400 operated at 30 Hz. The milling load was defined as the sum of the mass of the reactants per free volume in the jar and was equal to 10 mg/mL. All reactions using the vibratory ball mill were performed under air.

Mass spectra were recorded on a UPLCMS/MS system consisting of a Waters ACQUITY UPLC (Waters Corporation, Milford, MA, USA) coupled to a Waters TQD mass spectrometer (electrospray ionization mode ESI-tandem quadrupole). Chromatographic separations were carried out using the Acquity UPLC BEH (bridged ethyl hybrid) C18 column; 2.1 mm × 100 mm, and 1.7 µm particle size, equipped with Acquity UPLC BEH C18 Van Guard precolumn; 2.1 mm × 5 mm, and 1.7 µm particle size. The column was maintained at 40 °C and eluted under gradient conditions from 95% to 0% of eluent A over 10 min, at a flow rate of 0.3 mL min<sup>−1</sup>. Eluent A: water/formic acid (0.1%, *v/v*), Eluent B: acetonitrile/formic acid (0.1%, *v/v*).

<sup>1</sup>H and <sup>13</sup>C NMR spectra were recorded on a JEOL JNM-ECZR500 RS1 (ECZR version) at 500 and 126 MHz, respectively, and were reported in ppm using deuterated solvent for calibration (CDCl<sub>3</sub>). The *J* values were reported in hertz (Hz), and the splitting patterns were designated as follows: br s. (broad singlet), s (singlet), d (doublet), t (triplet), q (quartet), dd (doublet of doublets), ddd (doublet of doublet of doublets), m (multiplet).

#### 2.1.2. General Procedure A for Sulfonylation of Isoindoline Derivatives to Obtain Intermediates **2a–l**

Intermediates **1a–d** (1 eq), different fluoro-substituted benzenesulfonyl chloride (1.1 eq), and NaOH (3 eq) were introduced in a 35 mL SS jar (milling load 10 mg/mL) with one SS ball ( $\phi_{ball}$  = 1.5 cm). The reaction was carried out for 5–7 min at rt. The mixture was transferred into a filtration funnel, washed with distilled water, and dried under reduced pressure yielding intermediate **2a–l** in high yields (85–98%).

#### 2.1.3. General Procedure B for Aromatic Substitution to Obtain Final Compounds **3a–l**

Intermediates **2a–l** (1 eq) and anhydrous piperazine (3 eq) were introduced in a 10 mL SS jar (milling load 10 mg/mL) with one stainless steel ball ( $\phi_{ball}$  = 1.5 cm) followed by the addition of MeCN (34 µL,  $\eta$  = 0.4 µL mg<sup>−1</sup>) as a liquid assistant. The reaction was carried out for 1.5 h at 50 °C. In the case of intermediates **2e**, **2f**, **2g**, and **2h**, DMSO (42 µL,  $\eta$  = 0.4 µL mg<sup>−1</sup>) were used as a liquid additive, and the reactions were milled for 1.5 h at 80 °C. After the addition of cold water (5 mL), the resulting mixture was transferred into a filtration funnel, washed with distilled water, and dried under reduced pressure. The

products were purified via crystallization in ethanol, yielding final compounds **3a–l** as a white powder (yields 75–88%).

#### 2.1.4. General Procedure C for One-Pot Two-Step Reaction for Obtaining Compounds **3e**, **3f**, and **3g**

Isoindoline derivative (1 eq), sodium hydroxide (3 eq), and 3-fluorobenzenesulfonyl chloride (1.1 eq) were introduced in a 35 mL SS jar (milling load 10 mg/mL) with one stainless steel ball ( $\phi_{\text{ball}} = 1.5$  cm). After 10 min of milling at rt, anhydrous piperazine (3 eq) and DMSO (140  $\mu\text{L}$ ,  $\eta = 0.4 \mu\text{L mg}^{-1}$ ) were added into the jar, and the reaction was carried out for an additional 60 min at 80 °C. The resulting mixture was transferred into a filtration funnel, washed with distilled water, and dried under reduced pressure. The products were purified via crystallization in ethanol, yielding final compounds **3e**, **3f**, and **3g** as white powders (yields 85–88%).

#### 2.1.5. Characterization Data for Final Compounds

##### 2-[[4-(Piperazin-1-yl)phenyl]sulfonyl]isoindoline **3a**

White solid, 34 mg (isolated yield 88%) following procedure B; UPLC/MS purity 100%,  $t_R = 4.43$ ;  $\text{C}_{18}\text{H}_{21}\text{N}_3\text{O}_2\text{S}$ , MW 343.45, Monoisotopic Mass 343.14,  $[\text{M}+\text{H}]^+ 344.2$ .  $^1\text{H}$  NMR (500 MHz,  $\text{CDCl}_3$ )  $\delta$  ppm 1.70 (br s, 1H), 2.95–3.00 (m, 4H), 3.22–3.30 (m, 4H), 4.57 (s, 4H), 6.85–6.90 (m, 2H), 7.12–7.16 (m, 2H), 7.18–7.23 (m, 2H), 7.67–7.76 (m, 2H).  $^{13}\text{C}$  NMR (126 MHz,  $\text{DMSO}-d_6$ )  $\delta$  ppm 45.8, 48.0, 53.9, 113.9, 123.2, 123.3, 128.1, 129.7, 136.5, 154.5.

##### 4-Chloro-2-[[4-(piperazin-1-yl)phenyl]sulfonyl]isoindoline **3b**

White solid, 33 mg (isolated yield 81%) following procedure B; UPLC/MS purity 100%,  $t_R = 4.97$ ;  $\text{C}_{18}\text{H}_{20}\text{ClN}_3\text{O}_2\text{S}$ , MW 377.89, Monoisotopic Mass 377.10,  $[\text{M}+\text{H}]^+ 378.2$ .  $^1\text{H}$  NMR (500 MHz,  $\text{DMSO}-d_6$ )  $\delta$  ppm 2.73 (br s, 4H), 3.15 (br s, 4H), 4.45 (s, 2H), 4.55 (s, 2H), 6.96 (d,  $J = 8.9$  Hz, 2H), 7.16–7.29 (m, 3H), 7.61 (d,  $J = 8.9$  Hz, 2H).  $^{13}\text{C}$  NMR (126 MHz,  $\text{DMSO}-d_6$ )  $\delta$  ppm 45.8, 48.0, 53.4, 54.7, 113.9, 122.3, 122.9, 128.0, 128.2, 129.7, 130.4, 134.8, 139.1, 154.6.

##### 4-Bromo-2-[[4-(piperazin-1-yl)phenyl]sulfonyl]isoindoline **3c**

White solid 35 mg (isolated yield 80%) following procedure B; UPLC/MS purity 99%,  $t_R = 5.35$ ;  $\text{C}_{18}\text{H}_{20}\text{BrN}_3\text{O}_2\text{S}$ , MW 422.34, Monoisotopic Mass 421.05,  $[\text{M}+\text{H}]^+ 422.0/424.0$ .  $^1\text{H}$  NMR (500 MHz,  $\text{DMSO}-d_6$ )  $\delta$  ppm 2.68–2.80 (m, 4H), 3.10–3.21 (m, 4H), 4.40 (s, 2H), 4.58 (s, 2H), 6.97 (d,  $J = 9.2$  Hz, 2H), 7.16 (t,  $J = 8.6$  Hz, 1H), 7.22 (d,  $J = 9.2$  Hz, 1H), 7.39 (d,  $J = 7.7$  Hz, 1H), 7.61 (d,  $J = 8.9$  Hz, 2H).  $^{13}\text{C}$  NMR (126 MHz,  $\text{DMSO}-d_6$ )  $\delta$  ppm 45.8, 48.0, 54.9, 55.1, 113.9, 116.9, 122.8, 122.9, 129.7, 130.6, 130.9, 136.9, 138.8, 154.6.

##### 5-Bromo-2-[[4-(piperazin-1-yl)phenyl]sulfonyl]isoindoline **3d**

White solid, 36 mg (isolated yield 82%) following procedure B; UPLC/MS purity 100%,  $t_R = 5.18$ ;  $\text{C}_{18}\text{H}_{20}\text{BrN}_3\text{O}_2\text{S}$ , MW 422.34, Monoisotopic Mass 421.05,  $[\text{M}+\text{H}]^+ 422.1/424.1$ .  $^1\text{H}$  NMR (500 MHz,  $\text{DMSO}-d_6$ )  $\delta$  ppm 2.73 (br s, 4H), 3.15 (br s, 4H), 4.41 (s, 2H), 4.45 (s, 2H), 6.96 (d,  $J = 9.2$  Hz, 2H), 7.16 (d,  $J = 8.0$  Hz, 1H), 7.37 (d,  $J = 8.3$  Hz, 1H), 7.43 (s, 1H), 7.57 (d,  $J = 8.0$  Hz, 2H).  $^{13}\text{C}$  NMR (126 MHz,  $\text{DMSO}-d_6$ )  $\delta$  ppm 45.8, 48.0, 53.6, 113.9, 120.9, 123.0, 125.5, 126.4, 129.7, 130.9, 136.1, 139.4, 154.5.

##### 2-[[3-(Piperazin-1-yl)phenyl]sulfonyl]isoindoline **3e**

White solid, 137 mg (isolated yield 85%) following procedure C; UPLC/MS purity 100%,  $t_R = 4.52$ ;  $\text{C}_{18}\text{H}_{21}\text{N}_3\text{O}_2\text{S}$ , MW 343.45, Monoisotopic Mass 343.14,  $[\text{M}+\text{H}]^+ 344.2$ .  $^1\text{H}$  NMR (500 MHz,  $\text{CDCl}_3$ )  $\delta$  ppm 2.10 (br. s, 1H), 3.00–3.05 (m, 4H), 3.15–3.22 (m, 4H), 4.62 (s, 4H), 7.05 (ddd,  $J = 8.1, 2.5, 0.9$  Hz, 1H), 7.14–7.18 (m, 2H), 7.20–7.23 (m, 2H), 7.28–7.31 (m, 1H), 7.33–7.37 (m, 2H).  $^{13}\text{C}$  NMR (126 MHz,  $\text{CDCl}_3$ )  $\delta$  ppm 45.9, 49.6, 53.8, 114.0, 117.9, 119.7, 122.7, 127.8, 130.0, 136.2, 137.3, 152.2.

**4-Chloro-2-([3-(piperazin-1-yl)phenyl]sulfonyl)isoindoline 3f**

White solid, 145 mg (isolated yield 86%) following procedure C; UPLC/MS purity 99%,  $t_R = 5.08$ ;  $C_{18}H_{20}ClN_3O_2S$ , MW 377.89, Monoisotopic Mass 377.10,  $[M+H]^+$  378.2.  $^1H$  NMR (500 MHz,  $CDCl_3$ )  $\delta$  ppm 2.12 (br s, 1H), 2.99–3.08 (m, 4H), 3.15–3.25 (m, 4H), 4.63 (s, 2H), 4.67 (s, 2H), 7.01–7.09 (m, 2H), 7.14–7.21 (m, 2H), 7.27–7.31 (m, 1H), 7.32–7.40 (m, 2H).  $^{13}C$  NMR (126 MHz,  $CDCl_3$ )  $\delta$  ppm 45.9, 49.5, 53.5, 54.5, 113.9, 117.8, 119.8, 120.9, 127.8, 129.1, 129.5, 130.1, 135.1, 137.3, 138.1, 152.2.

**4-Bromo-2-([3-(piperazin-1-yl)phenyl]sulfonyl)isoindoline 3g**

White solid, 133 mg (isolated yield 88%) following procedure C; UPLC/MS purity 100%,  $t_R = 5.17$ ;  $C_{18}H_{20}BrN_3O_2S$ , MW 422.34, Monoisotopic Mass 421.05,  $[M+H]^+$  422.0/424.0.  $^1H$  NMR (500 MHz,  $DMSO-d_6$ )  $\delta$  ppm 2.77 (br s, 4H), 3.04 (br s, 4H), 4.48 (s, 2H), 4.66 (s, 2H), 7.16 (t,  $J = 5.7$  Hz, 4H), 7.22 (d,  $J = 8.0$  Hz, 2H), 7.33–7.45 (m, 2H).  $^{13}C$  NMR (126 MHz,  $DMSO-d_6$ )  $\delta$  ppm 45.9, 49.2, 55.0, 55.2, 112.7, 116.9, 117.2, 120.0, 122.8, 130.6, 130.7, 130.9, 136.8, 136.9, 138.8, 152.5.

**5-Bromo-2-([3-(piperazin-1-yl)phenyl]sulfonyl)isoindoline 3h**

White solid, 33 mg (isolated yield 76%) following procedure B; UPLC/MS purity 100%,  $t_R = 5.23$ ;  $C_{18}H_{20}BrN_3O_2S$ , MW 422.34, Monoisotopic Mass 421.05,  $[M+H]^+$  422.1/424.1.  $^1H$  NMR (500 MHz,  $DMSO-d_6$ )  $\delta$  ppm 2.77 (br s, 4H), 3.04 (br s, 4H), 4.47 (s, 2H), 4.52 (s, 2H), 7.10–7.25 (m, 4H), 7.33–7.41 (m, 2H), 7.43 (s, 1H).  $^{13}C$  NMR (126 MHz,  $DMSO-d_6$ )  $\delta$  ppm 45.9, 49.1, 53.6, 53.7, 112.8, 117.2, 120.0, 121.0, 125.5, 126.4, 130.6, 130.9, 136.0, 136.9, 139.3, 152.5.

**2-([2-(Piperazin-1-yl)phenyl]sulfonyl)isoindoline 3i**

White solid, 33 mg (isolated yield 84%) following procedure B; UPLC/MS purity 100%,  $t_R = 4.59$ ;  $C_{18}H_{21}N_3O_2S$ , MW 343.45, Monoisotopic Mass 343.14,  $[M+H]^+$  344.3.  $^1H$  NMR (500 MHz,  $CDCl_3$ )  $\delta$  ppm 1.91 (br.s, 1H), 2.90 (t,  $J = 4.3$  Hz, 4H), 3.03 (t,  $J = 4.6$  Hz, 4H), 4.82 (s, 4H), 7.13–7.16 (m, 2H), 7.19–7.23 (m, 3H), 7.28–7.31 (m, 1H), 7.44–7.53 (m, 1H), 8.02 (dd,  $J = 8.0, 1.7$  Hz, 1H).  $^{13}C$  NMR (126 MHz,  $CDCl_3$ )  $\delta$  ppm 46.1, 54.1, 55.3, 122.6, 123.8, 124.8, 127.6, 132.2, 134.0, 134.4, 136.6, 153.2.

**4-Chloro-2-([2-(piperazin-1-yl)phenyl]sulfonyl)isoindoline 3j**

White solid, 37 mg (isolated yield 83%) following procedure B; UPLC/MS purity 99%,  $t_R = 5.09$ ;  $C_{18}H_{20}ClN_3O_2S$ , MW 377.89, Monoisotopic Mass 377.10,  $[M+H]^+$  378.2.  $^1H$  NMR (500 MHz,  $CDCl_3$ )  $\delta$  ppm 2.55–2.62 (m, 1H), 2.93–3.00 (m, 4H), 3.09 (t,  $J = 4.3$  Hz, 4H), 4.80–4.85 (m, 2H), 4.85–4.88 (m, 2H), 6.97–7.10 (m, 1H), 7.14–7.20 (m, 2H), 7.21–7.25 (m, 1H), 7.32 (dd,  $J = 8.0, 1.1$  Hz, 1H), 7.48–7.54 (m, 1H), 8.02 (dd,  $J = 8.0, 1.7$  Hz, 1H).  $^{13}C$  NMR (126 MHz,  $CDCl_3$ )  $\delta$  ppm 45.9, 53.7, 54.7, 55.0, 120.8, 123.9, 125.0, 127.7, 129.0, 129.4, 132.2, 134.1, 134.2, 135.4, 138.4, 152.9.

**4-Bromo-2-([2-(piperazin-1-yl)phenyl]sulfonyl)isoindoline 3k**

White solid, 38 mg (isolated yield 88%) following procedure B; UPLC/MS purity 100%,  $t_R = 5.25$ ;  $C_{18}H_{20}BrN_3O_2S$ , MW 422.34, Monoisotopic Mass 421.05,  $[M+H]^+$  422.1/424.1.  $^1H$  NMR (500 MHz,  $DMSO-d_6$ )  $\delta$  ppm 2.77 (t,  $J = 4.6$  Hz, 4H), 3.19 (t,  $J = 4.9$  Hz, 4H), 4.40 (s, 2H), 4.58 (s, 2H), 6.98 (d,  $J = 9.2$  Hz, 2H), 7.17 (t,  $J = 7.7$  Hz, 1H), 7.22 (d,  $J = 7.2$  Hz, 1H), 7.40 (d,  $J = 8.6$  Hz, 1H), 7.59–7.64 (m, 2H).  $^{13}C$  NMR (126 MHz,  $DMSO-d_6$ )  $\delta$  ppm 45.5, 47.6, 54.9, 55.1, 114.0, 116.9, 122.8, 123.1, 129.7, 130.6, 130.9, 136.9, 138.8, 154.4.

**5-Bromo-2-([2-(piperazin-1-yl)phenyl]sulfonyl)isoindoline 3l**

White solid, 37 mg (isolated yield 86%) following procedure B; UPLC/MS purity 100%,  $t_R = 5.28$ ;  $C_{18}H_{20}BrN_3O_2S$ , MW 422.34, Monoisotopic Mass 421.05,  $[M+H]^+$  422.1/424.1.  $^1H$  NMR (500 MHz,  $DMSO-d_6$ )  $\delta$  ppm 2.68 (t,  $J = 4.3$  Hz, 4H), 2.79 (t,  $J = 4.3$  Hz, 4H), 4.68 (s, 4H), 7.18 (d,  $J = 8.0$  Hz, 1H), 7.27 (t,  $J = 7.6$  Hz, 1H), 7.34–7.40 (m, 2H), 7.41–7.48 (m, 1H),

7.52–7.61 (m, 1H), 7.87 (dd,  $J = 8.0, 1.4$  Hz, 1H).  $^{13}\text{C}$  NMR (126 MHz,  $\text{DMSO}-d_6$ )  $\delta$  ppm 45.9, 53.7, 53.8, 55.5, 120.9, 124.7, 125.3, 125.4, 126.2, 130.8, 132.4, 133.8, 135.0, 136.4, 139.6, 153.6.

## 2.2. In Vitro Biological Evaluation

### 2.2.1. Radioligand Binding Assays

All experiments were performed in HEK-293 cells, which stably express the human 5-HT<sub>1A</sub>, 5-HT<sub>6</sub>, 5-HT<sub>7b</sub>, and D<sub>2L</sub> receptors, or using CHO-K1 cells expressing human serotonin 5-HT<sub>2A</sub> receptor, following the previously reported procedures [22–24]. For displacement studies, the following radioligands (PerkinElmer, USA) at given concentrations were used at: 2.5 nM [ $^3\text{H}$ ]-8-OH-DPAT (135.2 Ci/mmol); 1 nM [ $^3\text{H}$ ]-ketanserin (53.4 Ci/mmol); 2 nM [ $^3\text{H}$ ]-LSD (83.6 Ci/mmol); 0.8 nM [ $^3\text{H}$ ]-5-CT (39.2 Ci/mmol) or 2.5 nM [ $^3\text{H}$ ]-raclopride (76.0 Ci/mmol) for 5-HT<sub>1A</sub>, 5-HT<sub>2A</sub>, 5-HT<sub>6</sub>, 5-HT<sub>7b</sub> and D<sub>2L</sub> receptors, respectively. All tested compounds were evaluated in triplicate at 7 concentrations ( $10^{-10}$ – $10^{-4}$  M). The inhibition constants ( $K_i$ ) were calculated from the Cheng–Prusoff equation [25]. A detailed description is reported in the Supporting Information.

### 2.2.2. Impact of Evaluated Compounds on cAMP Production in 1321N1 Cells

The ability of compounds **3e**, **3f**, and **3g** to inhibit 5-CT-induced production of cAMP was assessed using 1321N1 cells expressing the human 5-HT<sub>6</sub>R (PerkinElmer) using previously described procedures [15,17]. The level of cAMP was measured using the LANCE cAMP detection kit (PerkinElmer) according to the manufacturer's protocol. TR-FRET (Time Resolved Fluorescence Resonance Energy Transfer) was detected by an Infinite M1000 Pro (Tecan) using instrument settings from the LANCE cAMP detection kit manual. Tested compounds were evaluated at 8 concentrations ( $10^{-11}$ – $10^{-4}$  M) in triplicate.  $K_b$  values were calculated from the Cheng–Prusoff equation [25]. A detailed description is reported in the Supporting Information.

### 2.2.3. Impact of Evaluated Compounds on cAMP Production Elicited by Constitutively Active 5-HT<sub>6</sub>R in NG108-15 Cells

The functional properties at Gs signaling of **3e**, **3f**, **3g**, and the prototypic inverse agonist SB-258585 were evaluated using NG108-15 cells transiently expressing 5-HT<sub>6</sub>R and the cAMP sensor CAMYEL (cAMP sensor using YFP-Epac-RLuc) [26]. We previously demonstrated that the 5-HT<sub>6</sub>R displays a high level of constitutive activity in this model. Changes in cyclic AMP levels upon exposure to increasing concentrations of the tested compounds were assessed by BRET (Bioluminescence Resonance Energy Transfer) measurement using a Mithras LB 940 plate reader (Berthold Technologies), as previously described [17]. A detailed description is reported in the Supporting Information.

### 2.2.4. Impact of Tested Compounds on Cdk5-Dependent Neurite Growth

The inverse agonist properties at Cdk5 signaling of **3e**, **3f**, **3g**, and the prototypic inverse agonist SB-258585 were evaluated in NG108-15 cells transiently expressing 5-HT<sub>6</sub>R by measuring neurite outgrowth, as previously reported. NG108-15 cells were transfected with plasmids encoding either cytosolic GFP or a GFP-tagged 5-HT<sub>6</sub>R and grown on glass coverslips for 6 h. Then, cells were treated with either vehicle or the evaluated compounds. Neurite growth was measured on cells imaged using an AxioImagerZ1 microscope equipped with epifluorescence (Zeiss) using the Neuron J plugin of the ImageJ software (NIH). A detailed description is reported in the Supporting Information.

### 2.2.5. In Vitro Assessment of Metabolic Stability

Metabolic stability studies were performed according to reported protocols [27,28]. Evaluated compounds **3e**, **3f**, and **3g** at the final concentration of 20  $\mu\text{M}$  were preincubated in phosphate buffer (pH = 7.4), containing rat liver microsomes (microsome from rat male liver, pooled; 0.5 mg/mL; Merck/Millipore Sigma, Darmstadt, Germany, St. for 10 min at 37 °C. The reaction was initiated by adding the NADPH-regenerating system. After



0, 30, and 60 min, reactions were quenched with ice-cold methanol containing internal standard (pentoxifylline @ 100 nM). Next, samples were centrifuged, and the supernatants were analyzed by UPLC/MS.  $T_{1/2}$  was determined from the slope of the line on  $\ln$  (%remaining of parent compounds) vs. time plots.  $Cl_{int}$  was calculated from the equation:  $Cl_{int} = [\text{volume of incubation } (\mu\text{L}) / \text{amount of protein (mg)} \times 0.693] / t_{1/2}$ . All samples were analyzed in duplicate. The assay performance was confirmed by using extensive or low metabolized drugs as references (Imipramine and Donepezil, respectively).

#### 2.2.6. In Vitro Cytotoxicity Evaluation

Hepatotoxicity, neurotoxicity, and glial cytotoxicity were investigated using the following cellular models: human hepatocellular carcinoma (HepG2), human neuroblastoma (SHSY-5Y), and mouse astrocytes (C8-D1A), all from ATCC (American Type Culture Collection, Manassas, VA, USA). Cells were cultured in appropriate culture media recommended by ATCC supplemented with 10% fetal bovine serum (FBS; Gibco, Life Technologies, Carlsbad, CA, USA) and 1% antibiotic mixture (Gibco, Life Technologies, Carlsbad, CA, USA). Cells were cultured at standard conditions (5%  $\text{CO}_2$ , 95% humidity, 37 °C). For cytotoxicity experiments, cells were seeded into 96 well plates at an initial density of 2000 cells/well. After overnight incubation, cells were treated with **3e**, **3f**, and **3g** in a concentration range of 0.78–50  $\mu\text{M}$  for 48 h; then, an MTT assay was performed as described previously [17,29]. Briefly, following cell exposure, 10  $\mu\text{L}$  of MTT reagent was added to each well. After the next 4 h, the medium was aspirated, and formazan produced in cells appeared as dark crystals in the bottom of the wells. Next, 100  $\mu\text{L}$  DMSO was added to each well. Then, the optical density of the solution (OD) at 570 nm was determined on a plate reader (Spectra Max iD3, Molecular Devices, San Jose, CA, USA). The experiments were run three times in triplicates.

#### 2.2.7. In Vitro Assessment of Glioprotective Properties

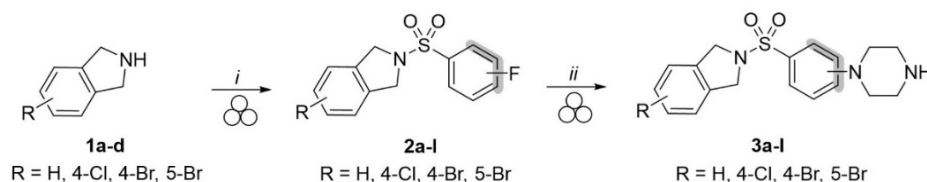
Mouse astrocytes (C8-D1A cell line, ATCC) were cultured in DMEM (Dulbecco's Modified Eagle's Medium) supplemented with 10% FBS (FBS; Gibco, Life Technologies, Carlsbad, CA, USA) and 1% antibiotic mixture (Gibco, Life Technologies, Carlsbad, CA, USA) at standard condition until the cells reached 80–90% confluence. Cells were harvested and seeded in 96-well plates at a density of 5000 cells/well. All experiments were conducted with a reduced amount of serum equal to 2.5%. The optimal amount of serum was determined experimentally on the basis of preliminary studies. After 24 h, cells were pre-incubated in the presence of compound **3g** or references CPPQ, SB-258585, and WAY-181187 (all at 0.25  $\mu\text{M}$ ). Then 6-OHDA (20  $\mu\text{M}$ ) or rotenone (0.5  $\mu\text{M}$ ) were added and co-incubated for the next 24 h. The ability of tested compounds to prevent 6-OHDA-induced or rotenone-induced cytotoxicity was assessed by MTT assay following the protocol described above. The experiments were run three times in triplicates.

### 3. Result and Discussion

#### 3.1. Mechanochemical Synthesis of Compounds **3a–3l**

A medicinal mechanochemical approach [28,30–32] was employed for the synthesis of a novel group of 1-(arylsulfonyl-isoindol-2-yl)piperazines **3a–3l** (Scheme 1). The optimization of the synthetic process started with the sulfonylation of unsubstituted isoindoline with the 4-fluorobenzenesulfonyl chloride (1.1 eq) (Table S1—SI). The reaction was initially performed in a 10 mL stainless-steel (SS) jar with a 1.5 cm diameter ball of the same material by using a vibratory ball mill (vbm) operated at 30 Hz. Potassium carbonate and sodium hydroxide guaranteed high conversions of reagents with a milling time of only 5 min. Although the use of potassium carbonate provided a better conversion rate, sodium hydroxide was chosen for further optimization due to its lower molecular weight. Increasing the amount of base from 2 to 3 equivalents resulted in full conversion to intermediate **2a** (isolated yield 98%). The reaction was then scaled up using a 35 mL SS jar without affecting the conversion or the yield (Table S1—SI). The optimized reaction conditions

for sulfonylation on a larger scale were then applied for the generation of intermediates **2b–2l**. Regardless of the substituent at the isoindoline scaffold and the kind of arylsulfonyl chloride, all intermediates **2a–2l** were obtained after a short milling time, ranging from 5 to 7 min. Of note, products **2a–2l** were isolated after filtration of the inorganic base, followed by washing the filtrate with water to provide desired compounds in high yields (85–98%).



**Scheme 1.** Mechanochemical synthesis of final compounds **3a–l** using vbm operating at 30 Hz. Reagents and conditions: (i)  $\phi_{ball} = 1.5$  cm, 35 mL SS jar, the total mass of reagents = 350 mg, milling load = 10 mg/mL; differently substituted isoindolines (1 eq), arylsulfonyl chloride (1.1 eq), NaOH (3 eq), 5–7 min, isolated yields (85–98%); (ii)  $\phi_{ball} = 1.5$  cm, 10 mL SS jar, the total mass of reagents = 85 mg, milling load = 10 mg/mL; sulfonylated intermediates **2a–l** (1 eq), anhydrous piperazine (3 eq), MeCN or DMSO ( $\eta = 0.4$   $\mu\text{L}/\text{mg}$ ), 50 or 80 °C, 1.5 h, isolated yields (75–88%).

Next, a mechanochemical procedure was applied to perform a nucleophilic aromatic substitution ( $S_NAr$ ) between fluorinated derivatives **2a–2l** and anhydrous piperazine to obtain final compounds **3a–3l**. The advantages of using temperature-controlled mechanochemical procedures have been recently demonstrated for different organic reactions [33–36]. In line with those findings, heating of a 10 mL SS jar containing intermediate **2a** (1 eq) and anhydrous piperazine (1 eq) at 50 °C for 1.5 h by using a temperature-controlled heat gun pre-set at 90 °C enabled the formation of the product **3a** (55% of conversion). No product was observed after milling of reagents at room temperature (Table S2—SI). Because the conversion rate was still not satisfactory, MeCN, a widely used aprotic polar solvent for  $S_NAr$  reactions in solution, was evaluated as a non-toxic liquid additive to enhance the overall mixing and reaction kinetics. Employing liquid-assisted grinding (LAG), in tandem with the increase in the amount of amine (3 eq of anhydrous piperazine), drastically improved the conversion rates up to 90% to furnish the desired product **3a** in 85% yield (Table S2—SI). Regardless of the kind of substituent at the isoindoline core, similar results were obtained with different 4-fluoro and 2-fluoro-containing substrates (isolated yields 80–88%). Despite the low reactivity of the fluorine atom in the 3-position with respect to sulfonamide moiety, optimization of reaction conditions was required. The replacement of MeCN with DMSO as a liquid additive enabled to increase the milling temperature of the jar to 80 °C (heat gun pre-set at 120 °C), providing final compounds **3e**, **3f**, **3g**, and **3h** in acceptable yields (75–78%). All the final compounds were isolated after simple precipitation from water followed by filtration to remove the excess of piperazine and crystallization in ethanol (Table S2—SI).

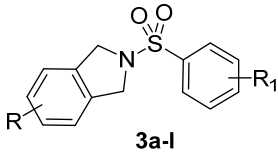
### 3.2. Radioligand Binding Assays in HEK-293 Cells and SAR Studies

All synthesized compounds were evaluated in  $^3\text{H}$ -LSD competition binding experiments for their affinity for 5-HT<sub>6</sub>R expressed in HEK-293 cells (Table 1). Embedding the sulfonamide moiety into an unsubstituted isoindoline scaffold was sufficient to provide potent compounds **3a** and **3e**. Compounds bearing the chlorine or bromine atom at the 4- or 5-position of isoindoline scaffold were equipotent (**3b** and **3c** vs. **3a**) or showed lower affinity than their unsubstituted analogs (**3d** vs. **3a** and **3l** vs. **3j**). Regardless of the kind of halogen at the isoindoline core, 3-piperazinyl derivatives **3e**, **3f**, **3g**, and **3h** were the most potent compounds ( $K_i < 5$  nM). A shift of the piperazine moiety from 3- to 4-position at the phenyl ring slightly decreased the affinity for the 5-HT<sub>6</sub>R but still provided high-affinity ligands **3a**, **3b**, and **3c**. In contrast, the introduction of piperazine moiety at the 2-position at the phenyl ring was not beneficial for the interaction with the 5-HT<sub>6</sub>R, as compounds **3i**, **3j** and **3l** were not active ( $K_i > 900$  nM). An exception, compound **3k** bearing the 4-bromo



substituent at the isoindoline scaffold, displayed average affinity at the 5-HT<sub>6</sub>R. This effect might result from the favorable localization of the bromine atom at the isoindoline fragment, which enabled compound **3k** to adopt an optimal position in the receptor binding pocket via the formation of hydrophobic/steric interactions.

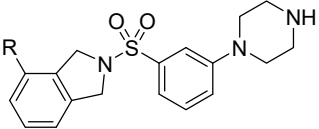
**Table 1.** The affinity of synthesized compounds **3a–l** and reference SB-258585 at the 5-HT<sub>6</sub>R.

 <b>3a–l</b>			
ID	R	R <sub>1</sub>	K <sub>i</sub> [nM] ± SEM <sup>a</sup>
<b>3a</b>	H	4-piperazinyl	6 ± 1
<b>3b</b>	4-Cl		7 ± 1
<b>3c</b>	4-Br		10 ± 2
<b>3d</b>	5-Br		87 ± 12
<b>3e</b>	H	3-piperazinyl	2 ± 0.8
<b>3f</b>	4-Cl		1 ± 0.2
<b>3g</b>	4-Br		1 ± 0.3
<b>3h</b>	5-Br		4 ± 0.5
<b>3i</b>	H	2-piperazinyl	977 ± 43
<b>3j</b>	4-Cl		918 ± 55
<b>3k</b>	4-Br		32 ± 5
<b>3l</b>	5-Br		1175 ± 99
<b>SB-258585<sup>b</sup></b>	-	-	8.9

<sup>a</sup> Mean K<sub>i</sub> values ± SEMs from three independent binding experiments in HEK293 cells; <sup>b</sup> Data taken from reference [20].

The most potent 5-HT<sub>6</sub>R ligands **3e**, **3f**, and **3g** bearing the piperazine moiety localized at position-3 at the sulfonamide fragment were then tested for their activity at serotonin 5-HT<sub>1A</sub>, 5-HT<sub>2A</sub>, 5-HT<sub>7</sub>, and dopaminergic D<sub>2</sub> receptors (Table 2). These compounds were highly selective over the off-target 5-HT<sub>7</sub>R and D<sub>2</sub>R (K<sub>i</sub> > 2 μM). They also displayed good selectivity toward the 5-HT<sub>1A</sub>R subtype (up to 680-folds). The selectivity index over the 5-HT<sub>2A</sub>R (K<sub>i</sub> < 200 nM) was still satisfactory.

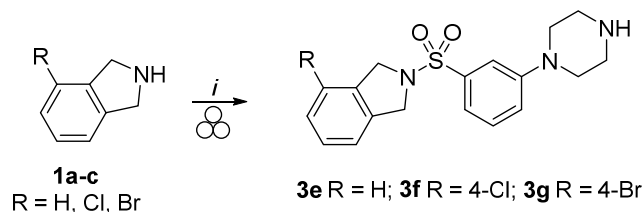
**Table 2.** The antagonist properties of selected compounds **3e**, **3f**, and **3g**, their impact on 5-HT<sub>6</sub>R constitutive activity, and their K<sub>i</sub> values for 5-HT<sub>6</sub>, 5-HT<sub>1A</sub>, 5-HT<sub>2A</sub>, 5-HT<sub>7</sub>, and D<sub>2</sub>Rs.

 <b>3e</b> R = H; <b>3f</b> R = 4-Cl; <b>3g</b> R = 4-Br							
ID	5-HT <sub>6</sub> R			K <sub>i</sub> [nM] <sup>a</sup>			
	K <sub>i</sub> [nM] <sup>a</sup>	K <sub>b</sub> [nM] <sup>b</sup>	Functional Profile at Gs Signaling <sup>c</sup>	5-HT <sub>1A</sub> R	5-HT <sub>2A</sub> R	5-HT <sub>7</sub> R	D <sub>2</sub>
<b>3e</b>	2 ± 0.2	0.7 ± 0.2	Neutral antagonist	951 ± 120	128 ± 37	4529 ± 327	3424 ± 415
<b>3f</b>	1 ± 0.2	3.5 ± 0.8	Neutral antagonist	385 ± 71	170 ± 32	10660 ± 1025	2026 ± 299
<b>3g</b>	1 ± 0.4	1.6 ± 0.3	Neutral antagonist	680 ± 33	159 ± 25	8798 ± 854	2440 ± 324
<b>SB-258585<sup>d</sup></b>	8.9	NT	Inverse agonist	645	1023	3388	3802

<sup>a</sup> Mean K<sub>i</sub> values ± SEMs from three independent binding experiments; <sup>b</sup> Mean K<sub>b</sub> values ± SEMs from three independent experiments in 1321N1 cells; <sup>c</sup> Data were obtained from four independent transfection experiments in NG108-15 cells and measured in triplicate; <sup>d</sup> Data taken from reference [20]; NT = not tested.

### 3.3. One-Pot Two-Step Mechanochemical Synthesis of Compounds **3e**, **3f**, and **3g**

To optimize the developed mechanochemical procedure, a one-pot, two-step protocol was employed for the synthesis of the most potent derivatives **3e**, **3f**, and **3g** (Scheme 2).



**Scheme 2.** One-pot two-step strategy for the mechanochemical synthesis of compounds **3e**, **3f**, and **3g** using vbm operating at 30 Hz. Reagents and conditions:  $\phi_{\text{ball}} = 1.5$  cm, 35 mL SS jar, the total mass of reagents = 350 mg, milling load = 10 mg/mL; differently substituted isoindolines (1 eq), 3-fluorobenzenesulfonyl chloride (1.1 eq), NaOH (3 eq), 10 min then anhydrous piperazine (3 eq), DMSO ( $\eta = 0.4$   $\mu\text{L}/\text{mg}$ ), 80  $^{\circ}\text{C}$ , 60 min (isolated yields 85–88%).

According to the newly elaborated protocol, intermediates generated upon milling the isoindolines **1a–c** (1 eq.) with 3-fluorobenzenesulfonyl chloride (1.1 eq) and NaOH (3 eq) were directly submitted to  $\text{S}_{\text{N}}\text{Ar}$  by the addition of anhydrous piperazine (3 eq) and DMSO ( $\eta = 0.4$   $\mu\text{L}/\text{mg}$ ) in the 35 mL SS jar (Scheme 2). The simplified one-pot two-step synthetic procedure enabled to obtain final compounds in higher overall yields (85–88%) when compared to the sequential two-step protocol (75–78%) by improving the conversion rates of the  $\text{S}_{\text{N}}\text{Ar}$  reaction. A possible explanation could be found in the role of NaOH in neutralizing the generated in situ HF, maintaining a favorable basic environment for the substitution reaction.

### 3.4. Antagonist Properties of Selected Compounds at 5-HT<sub>6</sub>R-Operated Gs Signaling

The antagonist properties of compounds **3e**, **3f**, and **3g** at 5-HT<sub>6</sub>R-operated Gs signaling were assessed in comparison with the reference ligand intepirdine and using 5-CT as an agonist in 1321N1 cells over-expressing the 5-HT<sub>6</sub>R (Figure 3A). Likewise, intepirdine ( $K_{\text{b}} = 1 \pm 0.4$  nM, Figure 3A), all compounds inhibited the 5-CT-stimulated cAMP accumulation and, thus, were classified as receptor antagonists ( $K_{\text{b}} = 0.7–6.9$  nM, Table 2).

Subsequently, the ability of compounds **3e**, **3f**, and **3g** to inhibit 5-HT<sub>6</sub>R constitutive activity were further investigated in neuroblastoma NG108-15 cells, in line with our previous observation indicating that transiently expressed receptors exhibit a high level of constitutive activity at Gs signaling in this cell population. Neither of the evaluated compounds significantly affected basal cAMP production in NG108-15 cells, indicating that they behave as neutral antagonists (Table 2, Figure 3B). In contrast and consistent with previous findings, the reference compound SB-258585 reduced the basal level of cAMP, showing inverse agonist properties [14].

In light of these findings and considering structure-functional activity relationships, it seems that the more flexible primary sulfonamide of SB-258585 provides a particular orientation of the aromatic fragment that allows inhibition of the spontaneously active conformation of 5-HT<sub>6</sub>R [20], while inversion of the sulfonamide and its concomitant incorporation into isoindoline scaffold confers neutral antagonist properties.

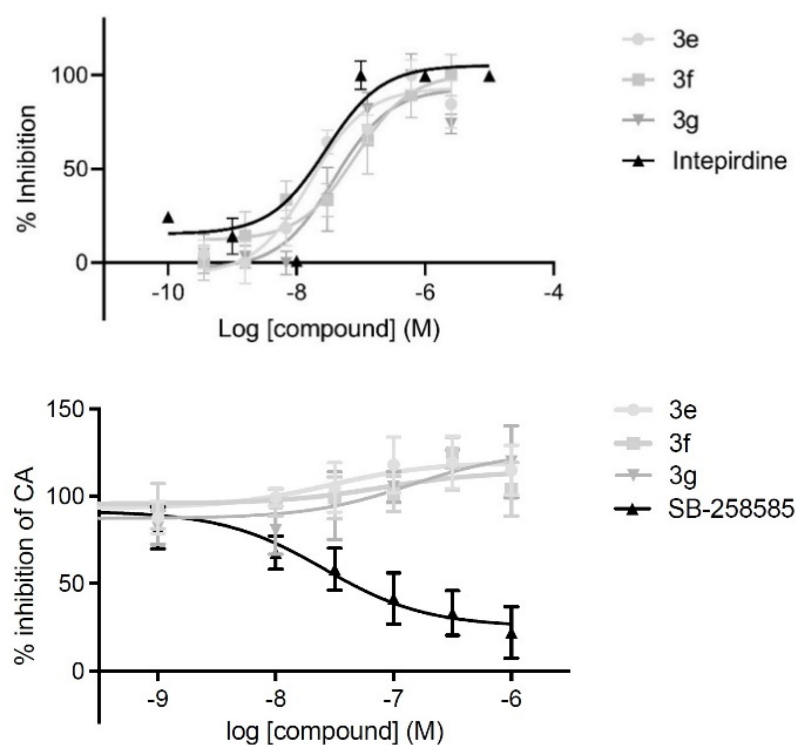


**Figure 3.** (A): Functional dose-response curve of inhibition of cAMP production at 5-HT<sub>6</sub>R for selected compounds **3e**, **3f**, and **3g** in 1321N1 cells. Data were obtained from three independent experiments run in triplicate. (B): Impact of compounds **3e**, **3f**, and **3g** and SB-258585 on basal cAMP production in NG108-15 cells transiently expressing 5-HT<sub>6</sub>R. For each compound, six independent transfection experiments were performed, and data were measured in triplicate. Data are given as means  $\pm$  SEM of the values.

Beyond the ability to adopt different conformational states able to recruit the canonical Gs-adenylyl cyclase pathway in the presence and absence of an agonist, 5-HT<sub>6</sub>R also activates Cdk5 signaling in an agonist-independent manner [21]. We previously showed that neurite growth in NG108-15 cells transiently expressing the 5-HT<sub>6</sub>R provides an in vitro model to assess agonist-independent activation of Cdk5 signaling, enabling pharmacological distinction between inverse agonists and neutral antagonists at Cdk5 signaling [21,37].

As previously observed, transient expression of the 5-HT<sub>6</sub>R in NG108-15 cells markedly increased neurite growth compared with cells expressing GFP alone. Treatment of NG108-15 cells expressing the receptor with compounds **3e**, **3f**, and **3g** for 24 h significantly reduced neurite length ( $11.81 \pm 2.61 \mu\text{m}$ ,  $n = 112$  neurites,  $10.92 \pm 0.89 \mu\text{m}$ ,  $n = 182$  neurites and  $8.08 \pm 0.84 \mu\text{m}$ ,  $n = 105$  neurites, respectively vs.  $16.95 \pm 1.5 \mu\text{m}$ ,  $n = 228$  neurites in vehicle-treated cells, Figure 4). Of note, compound **3g** was the most effective compound providing a 50% reduction in neurite growth slightly higher than that measured in cells treated with the reference SB-258585 ( $10.3 \pm 0.77 \mu\text{m}$ ,  $n = 182$  neurites). In this case, reducing the flexibility of the sulfonamide fragment of SB-258585 by its inversion and incorporation into isoindoline moiety did not impact the functional profile of tested compounds at the 5-HT<sub>6</sub>R-elicited Cdk5 pathway. To our knowledge, compound **3g** represents a unique example of a 5-HT<sub>6</sub>R ligand that behaves as a neutral antagonist at Gs signaling and displays potent inverse agonist properties at a non-canonical pathway engaged by the receptor.

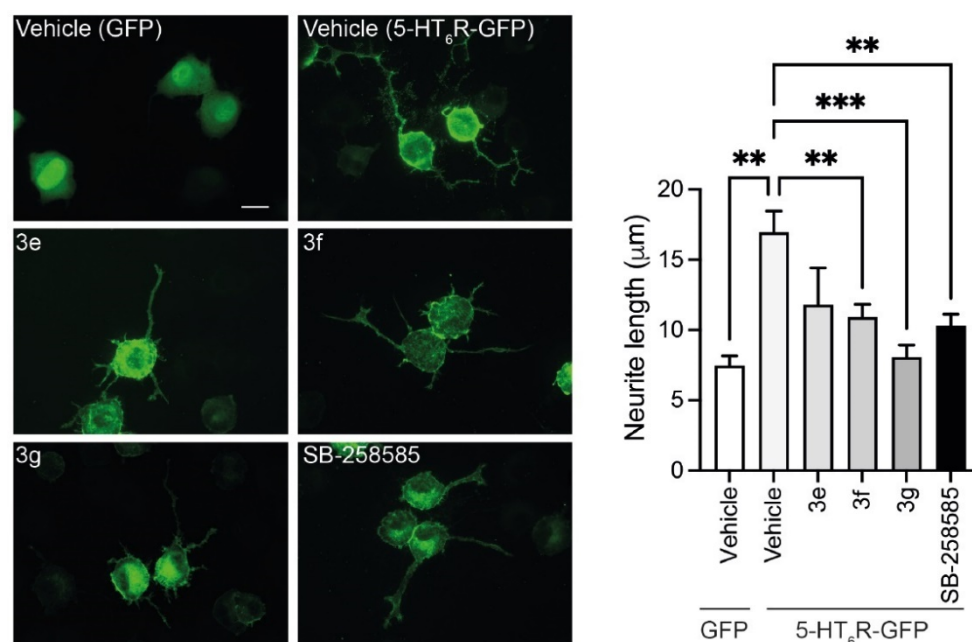


**Figure 4.** Impact of compounds **3e**, **3f**, **3g**, and SB-258585 on Cdk5 signaling pathway. NG108-15 cells were transfected with a plasmid encoding a GFP-tagged 5-HT<sub>6</sub>R or GFP alone. Cells expressing the receptor were exposed to vehicle (DMSO), compounds **3e**, **3f**, **3g**, and reference SB-2758585 for 48 h. The left panel shows representative images of cells in each condition (scale bar 20 μm). The histogram shows the mean ± SEM of values obtained from at least three independent experiments. \*\*\*  $p < 0.001$ , \*\*  $p < 0.02$  vs. cells expressing GFP. All groups were compared using one-way ANOVA followed by Tukey's multiple comparison test.

### 3.5. In Vitro Metabolic Stability and Preliminary Safety Assessment for **3e**, **3f**, and **3g**

Preliminary ADME/Tox properties of compounds **3e**, **3f**, and **3g** were screened using in vitro methods. First, biotransformation studies using rat liver microsomes (RLM) revealed that all tested compounds were metabolically stable (Table 3). Unsubstituted derivative **3e** displayed a lower clearance value ( $Cl_{int} = 3.78 \mu\text{L}/\text{min}/\text{mg}$ ) than its halogenated analogs **3f** (4-Cl) and **3g** (4-Br), similar to that of the reference drug donepezil ( $Cl_{int} = 3.65 \mu\text{L}/\text{min}/\text{mg}$ ). Imipramine, an extensively metabolized drug used as a positive control, displayed much higher clearance ( $Cl_{int} = 115.65 \mu\text{L}/\text{min}/\text{mg}$ ).

**Table 3.** Preliminary metabolic stability and safety profile for compounds **3e**, **3f**, and **3g**.

ID	Metabolic Stability <sup>a</sup>			Cytotoxicity <sup>b</sup>		
	$t_{1/2}$ [min]	$Cl_{int}$ [ $\mu\text{L}/\text{min}/\text{mg}$ ]	Major Metabolite	HepG2	SH-SY5Y	C8-D1A
<b>3e</b>	367	3.78	not detected	$IC_{50} > 50 \mu\text{M}$	$IC_{50} = 42 \mu\text{M}$	$IC_{50} > 50 \mu\text{M}$
<b>3f</b>	76.95	18.01	hydroxylated	$IC_{50} > 50 \mu\text{M}$	$IC_{50} = 38 \mu\text{M}$	$IC_{50} > 50 \mu\text{M}$
<b>3g</b>	94.41	14.68	hydroxylated	$IC_{50} > 50 \mu\text{M}$	$IC_{50} = 48 \mu\text{M}$	$IC_{50} > 50 \mu\text{M}$
Donepezil	379	3.65	not detected	NT	NT	NT
Imipramine	11.98	115.65	Des-methylated	NT	NT	NT
Doxorubicin	NT	NT	NT	$IC_{50} = 10.8 \mu\text{M}$	$IC_{50} = 4.4 \mu\text{M}$	$IC_{50} = 12.3 \mu\text{M}$

<sup>a</sup> Determined in the RLM test, at a protein concentration of 0.5 mg/mL; <sup>b</sup> Results were obtained upon treatment of HepG2, SH-SY5Y, and C8-D1A cells for 48 h using MTT test; data from three independent experiments; NT = not tested.

Then, to exclude potential cytotoxic effects, compounds **3e**, **3f**, and **3g** were tested in human hepatocellular carcinoma (HepG2), human neuroblastoma (SH-SY5Y), and mouse astrocytes (C8-D1A). None of the evaluated compounds affected the metabolic activity

of cells, as assessed by the MTT (3-[4,5-dimethylthiazol-2-yl]-2,5-diphenyl tetrazolium bromide) test. None of them induced any hepatotoxic, neurotoxic, or gliotoxic activity at a concentration of 25  $\mu$ M (Table 3), in contrast to doxorubicin used as a positive control, which displayed high cytotoxic effects ( $IC_{50}$  = 4.4, 10.8 and 12.3  $\mu$ M against SH-SY5Y, HepG2 and C8-D1A cells, respectively).

### 3.6. Glioprotective Properties of Compound 3g

Considering the pivotal physiological role of astrocytes in contrasting oxidative stress and promoting tissue repair [38,39], supporting their neuroprotective function might be regarded as a tangible strategy to improve the current therapeutic needs in the treatment of neurodegenerative disorders. We next investigated the ability of compound **3g** to protect astrocytes against 6-OHDA- and ROT-induced cytotoxicity in C8-D1A cells, in line with our previous findings indicating that blocking of 5-HT<sub>6</sub>R results in glioprotective effect against toxic insults [17,40]. In comparison, we assessed the effect of WAY-181187, a 5-HT<sub>6</sub>R agonist, SB-258585, an inverse agonist, and CPPQ, a neutral antagonist [18]. For this purpose, cells were co-incubated with the evaluated compounds (at the non-toxic concentration of 0.25  $\mu$ M) and 6-OHDA or ROT (20 and 0.5  $\mu$ M, respectively). After 24 h of incubation, the viability of astrocytes was determined using the MTT assay.

Both compound **3g** and CPPQ, which behave as neutral antagonists at the 5-HT<sub>6</sub>R-operated Gs signaling pathway, decreased the cytotoxicity of 6-OHDA and ROT in C8-D1A astrocytes (Figure 5A,B), whereas the inverse agonist SB-258585 did not evoke any protective effect. Likewise, treatment of C8-D1A cells with WAY-181187, a 5-HT<sub>6</sub>R agonist, slightly but not significantly enhanced the gliotoxic effects of 6-OHDA and ROT. These findings suggest that 5-HT<sub>6</sub>R activation by 5-HT contained in the serum from the cell-growing medium contributes to the toxicity of 6-OHDA and rotenone in C8-D1A astrocytes.

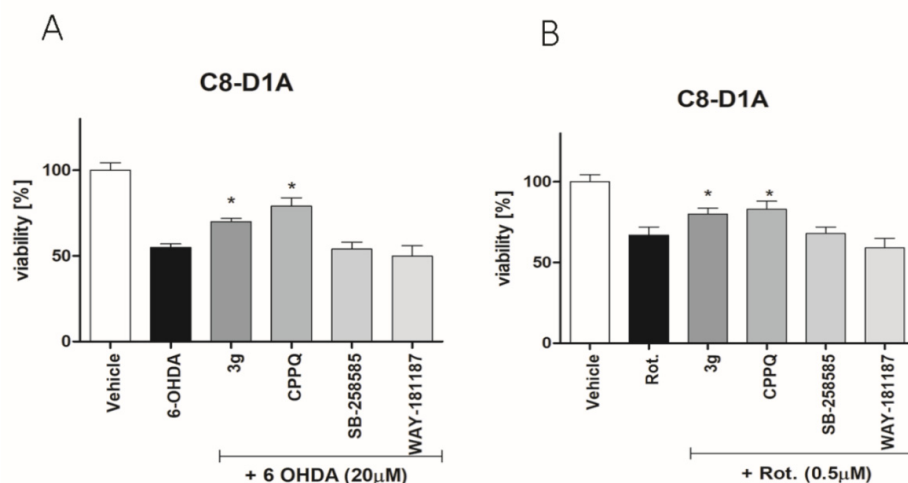


**Figure 5.** Effect of **3g** and CPPQ (neutral antagonists), SB-258585 (inverse agonist), and WAY-181187 (agonist) upon 6-OHDA- (A) or ROT- (B) induced toxicity in C8-D1A astrocyte cell line. Twenty-four hours after the onset of 6-OHDA or ROT treatment, cells were co-incubated with either vehicle or tested compounds (all at 0.25  $\mu$ M) and 6-OHDA (20  $\mu$ M) or ROT (0.5  $\mu$ M) for an additional 24 h period. Graphs present the means  $\pm$  SD. \*  $p$  < 0.05 vs. cells treated with cytotoxic agents (6-OHDA or ROT) using the Mann–Whitney test.

## 4. Conclusions

Structural modifications around the sulfonamide moiety of SB-258585 led to the design of 1-(arylsulfonyl-isoindol-2-yl)piperazines as a new framework for developing biased 5-HT<sub>6</sub>R ligands. An application of a one-pot two-step mechanochemical procedure enabled the synthesis of selected derivatives in a fast and efficient manner (isolated yields 85–88%). Tested compounds displayed high metabolic stability in RLM assays and no toxic effect



toward human hepatocellular carcinoma and neuroblastoma or a mouse astrocyte cell line. In vitro functional evaluation identified compounds that behave as potent neutral antagonists at 5-HT<sub>6</sub>R-elicited Gs signaling and simultaneously display inverse agonist properties at the Cdk5 pathway. These findings underline the important role of the sulfonamide moiety, in particular its inversion and rigidification, for the design of biased ligands at 5-HT<sub>6</sub>R-operated Gs and Cdk5 signaling pathways. Moreover, the neutral antagonists **3g** and CPPQ exerted glioprotective properties against 6-OHDA- and ROT-induced toxicity in the C8-D1A astrocyte cell line. In contrast, no protective effect and even a slight increase in cytotoxicity were observed upon treatment with the inverse agonist SB-258585 or the agonist WAY-181187, respectively. The identified biased ligand **3g** might be considered as a molecular probe to explore the role of 5-HT<sub>6</sub>R in neurodegenerative diseases further.

**Supplementary Materials:** The following supporting information can be downloaded at: <https://www.mdpi.com/article/10.3390/biom13010012/s1>. Characterization of all intermediates; UPLC-MS, <sup>1</sup>H-NMR, and <sup>13</sup>C-NMR of all intermediates and final compounds; Table S1–S1: Optimization of milling conditions for sulfonylation of isoindolines 1a–d; Table S2–S1: Optimization of milling conditions for S<sub>N</sub>Ar of intermediates 2a–l; Figure S1–S1: The effect of compound 3g on cellular viability.

**Author Contributions:** Conceptualization: V.C. and P.Z.; synthesis: V.C. and W.T.; characterization: W.T.; in vitro pharmacological studies: S.C.-D., G.S. and O.B.; metabolic stability: V.C. and K.B.-F.; safety assessment and glioprotective evaluation: P.K.-A.; validation and data analysis: X.B., E.P., A.J.B., F.L., P.M. and P.Z.; manuscript writing, review and editing: V.C., S.C.-D., P.M., and P.Z. All authors have read and agreed to the published version of the manuscript.

**Funding:** The project was financially supported by the National Science Center, Poland, grant no. DEC-2021/05/X/NZ7/01847, by the French National Research Agency, grant no. ANR-16-IDEX-0006, and by the Priority Research Area qLife under the program “Excellence Initiative Research University” at the Jagiellonian University in Krakow.

**Institutional Review Board Statement:** Not applicable.

**Informed Consent Statement:** Not applicable.

**Data Availability Statement:** The data presented in this study are available in the Supplementary Materials.

**Conflicts of Interest:** The authors declare no conflict of interest.

**Sample Availability:** Samples of the compounds are available from the authors.

## Abbreviations

ADMET (Absorption, Distribution, Metabolism, Excretion, and Toxicity); SEM (Standard Error of Mean); MeCN (Acetonitrile), DMSO (Dimethylsulfoxide), 5-CT (5-carboxamidotryptamine); cAMP (cyclic adenosine-monophosphate).

## References

1. Barnes, N.M.; Ahern, G.P.; Becamel, C.; Bockaert, J.; Camilleri, M.; Chaumont-Dubel, S.; Claeysen, S.; Cunningham, K.A.; Fone, K.C.; Gershon, M.; et al. International Union of Basic and Clinical Pharmacology. CX. Classification of Receptors for 5-Hydroxytryptamine; Pharmacology and Function. *Pharmacol. Rev.* **2021**, *73*, 310–520. [CrossRef] [PubMed]
2. Zajdel, P.; Marciniak, K.; Satała, G.; Canale, V.; Kos, T.; Partyka, A.; Jastrzębska-Więsek, M.; Wesołowska, A.; Basińska-Ziobroń, A.; Wójcikowski, J.; et al. N<sub>1</sub>-Azinylsulfonyl-1H-indoles: 5-HT<sub>6</sub> Receptor Antagonists With Procognitive and Antidepressant-Like Properties. *ACS Med. Chem. Lett.* **2016**, *7*, 618–622. [CrossRef] [PubMed]
3. Hogendorf, A.S.; Hogendorf, A.; Kurczab, R.; Kalinowska-Tłuścik, J.; Popik, P.; Nikiforuk, A.; Krawczyk, M.; Satała, G.; Lenda, T.; Knutelska, J.; et al. 2-Aminoimidazole-Based Antagonists of the 5-HT(6) Receptor—A New Concept in Aminergic GPCR Ligand Design. *Eur. J. Med. Chem.* **2019**, *179*, 1–15. [CrossRef] [PubMed]
4. Nirogi, R.; Abraham, R.; Benade, V.; Medapati, R.B.; Jayarajan, P.; Bhyrapuneni, G.; Muddana, N.; Mekala, V.R.; Subramanian, R.; Shinde, A.; et al. SUVN-502, a Novel, Potent, Pure, and Orally Active 5-HT<sub>6</sub> Receptor Antagonist: Pharmacological, Behavioral, and Neurochemical Characterization. *Behav. Pharmacol.* **2019**, *30*, 16–35. [CrossRef]

5. Sudoł, S.; Cios, A.; Jastrzębska-Więsek, M.; Honkisz-Orzechowska, E.; Mordyl, B.; Wilczyńska-Zawal, N.; Satała, G.; Kucwaj-Brysz, K.; Partyka, A.; Latacz, G.; et al. The Phenoxyalkyltriazine Antagonists for 5-HT(6) Receptor with Promising Procognitive and Pharmacokinetic Properties In Vivo in Search for a Novel Therapeutic Approach to Dementia Diseases. *Int. J. Mol. Sci.* **2021**, *22*, 10773. [\[CrossRef\]](#)
6. Zajdel, P.; Grychowska, K.; Mogilski, S.; Kurczab, R.; Satała, G.; Bugno, R.; Kos, T.; Gołębiowska, J.; Malikowska-Racia, N.; Nikiforuk, A.; et al. Structure-Based Design and Optimization of FPPQ, a Dual-Acting 5-HT(3) and 5-HT(6) Receptor Antagonist with Antipsychotic and Procognitive Properties. *J. Med. Chem.* **2021**, *64*, 13279–13298. [\[CrossRef\]](#)
7. Dayer, A.G.; Jacobshagen, M.; Chaumont-Dubel, S.; Marin, P. 5-HT<sub>6</sub> Receptor: A New Player Controlling the Development of Neural Circuits. *ACS Chem. Neurosci.* **2015**, *6*, 951–960. [\[CrossRef\]](#)
8. Pujol, C.N.; Dupuy, V.; Séveno, M.; Runtz, L.; Bockaert, J.; Marin, P.; Chaumont-Dubel, S. Dynamic Interactions of the 5-HT<sub>6</sub> Receptor with Protein Partners Control Dendritic Tree Morphogenesis. *Sci. Signal.* **2020**, *13*, eaax9520. [\[CrossRef\]](#)
9. Sheu, S.-H.; Upadhyayula, S.; Dupuy, V.; Pang, S.; Deng, F.; Wan, J.; Walpita, D.; Pasolli, H.A.; Houser, J.; Sanchez-Martinez, S.; et al. A Serotonergic Axon-Cilium Synapse Drives Nuclear Signaling to Alter Chromatin Accessibility. *Cell* **2022**, *185*, 3390–3407. [\[CrossRef\]](#)
10. De Deurwaerdere, P.; Bharatiya, R.; Chagraoui, A.; Di Giovanni, G. Constitutive Activity of 5-HT Receptors: Factual Analysis. *Neuropharmacology* **2020**, *168*, 107967. [\[CrossRef\]](#)
11. Berthouex, C.; Hamieh, A.M.; Rogliardo, A.; Doucet, E.L.; Coudert, C.; Ango, F.; Grychowska, K.; Chaumont-Dubel, S.; Zajdel, P.; Maldonado, R.; et al. Early 5-HT(6) Receptor Blockade Prevents Symptom Onset in a Model of Adolescent Cannabis Abuse. *EMBO Mol. Med.* **2020**, *12*, e10605. [\[CrossRef\]](#) [\[PubMed\]](#)
12. Doucet, E.; Grychowska, K.; Zajdel, P.; Bockaert, J.; Marin, P.; Bécamel, C. Blockade of Serotonin 5-HT(6) Receptor Constitutive Activity Alleviates Cognitive Deficits in a Preclinical Model of Neurofibromatosis Type 1. *Int. J. Mol. Sci.* **2021**, *22*, 10178. [\[CrossRef\]](#) [\[PubMed\]](#)
13. Deraredj Nadim, W.; Chaumont-Dubel, S.; Madouri, F.; Cobret, L.; De Tauzia, M.-L.; Zajdel, P.; Bénédicti, H.; Marin, P.; Morisset-Lopez, S. Physical Interaction Between Neurofibromin and Serotonin 5-HT<sub>6</sub> Receptor Promotes Receptor Constitutive Activity. *Proc. Natl. Acad. Sci. USA* **2016**, *113*, 12310–12315. [\[CrossRef\]](#)
14. Martin, P.-Y.; Doly, S.; Hamieh, A.M.; Chapuy, E.; Canale, V.; Drop, M.; Chaumont-Dubel, S.; Bantreil, X.; Lamaty, F.; Bojarski, A.J.; et al. mTOR Activation by Constitutively Active Serotonin<sub>6</sub> Receptors as New Paradigm in Neuropathic Pain and its Treatment. *Prog. Neurobiol.* **2020**, *193*, 101846. [\[CrossRef\]](#) [\[PubMed\]](#)
15. Drop, M.; Jacquot, F.; Canale, V.; Chaumont-Dubel, S.; Walczak, M.; Satała, G.; Nosalska, K.; Mahoro, G.U.; Słoczyńska, K.; Piska, K.; et al. Neuropathic Pain-Alleviating Activity of Novel 5-HT(6) Receptor Inverse Agonists derived from 2-aryl-1H-pyrrole-3-carboxamide. *Bioorg. Chem.* **2021**, *115*, 105218. [\[CrossRef\]](#) [\[PubMed\]](#)
16. Vanda, D.; Soural, M.; Canale, V.; Chaumont-Dubel, S.; Satała, G.; Kos, T.; Funk, P.; Fülöpová, V.; Lemrová, B.; Koczurkiewicz, P.; et al. Novel Non-Sulfonamide 5-HT(6) Receptor Partial Inverse Agonist in a Group of Imidazo[4,5-*b*]pyridines With Cognition Enhancing Properties. *Eur. J. Med. Chem.* **2018**, *144*, 716–729. [\[CrossRef\]](#)
17. Vanda, D.; Canale, V.; Chaumont-Dubel, S.; Kurczab, R.; Satała, G.; Koczurkiewicz-Adamczyk, P.; Krawczyk, M.; Pietruś, W.; Blicharz, K.; Pękala, E.; et al. Imidazopyridine-Based 5-HT(6) Receptor Neutral Antagonists: Impact of N(1)-Benzyl and N(1)-Phenylsulfonyl Fragments on Different Receptor Conformational States. *J. Med. Chem.* **2021**, *64*, 1180–1196. [\[CrossRef\]](#) [\[PubMed\]](#)
18. Grychowska, K.; Satała, G.; Kos, T.; Partyka, A.; Colacino, E.; Chaumont-Dubel, S.; Bantreil, X.; Wesołowska, A.; Pawłowski, M.; Martinez, J.; et al. Novel 1H-Pyrrolo[3,2-*c*]quinoline Based 5-HT<sub>6</sub> Receptor Antagonists with Potential Application for the Treatment of Cognitive Disorders Associated with Alzheimer's Disease. *ACS Chem. Neurosci.* **2016**, *7*, 972–983. [\[CrossRef\]](#)
19. Drop, M.; Canale, V.; Chaumont-Dubel, S.; Kurczab, R.; Satała, G.; Bantreil, X.; Walczak, M.; Koczurkiewicz-Adamczyk, P.; Latacz, G.; Gwizdak, A.; et al. 2-Phenyl-1H-pyrrole-3-carboxamide as a New Scaffold for Developing 5-HT(6) Receptor Inverse Agonists with Cognition Enhancing Activity. *ACS Chem. Neurosci.* **2021**, *12*, 1228–1240. [\[CrossRef\]](#)
20. Hirst, W.D.; Minton, J.A.; Bromidge, S.M.; Moss, S.F.; Latter, A.J.; Riley, G.; Routledge, C.; Middlemiss, D.N.; Price, G.W. Characterization of [(125)I]-SB-258585 Binding to human Recombinant and Native 5-HT(6) Receptors in Rat, Pig and Human Brain Tissue. *Br. J. Pharmacol.* **2000**, *130*, 1597–1605. [\[CrossRef\]](#)
21. Duhr, F.; Délérès, P.; Raynaud, F.; Séveno, M.; Morisset-Lopez, S.; Mannoury la Cour, C.; Millan, M.J.; Bockaert, J.; Marin, P.; Chaumont-Dubel, S. Cdk5 Induces Constitutive Activation of 5-HT<sub>6</sub> Receptors to Promote Neurite Growth. *Nat. Chem. Biol.* **2014**, *10*, 590–597. [\[CrossRef\]](#) [\[PubMed\]](#)
22. Partyka, A.; Kurczab, R.; Canale, V.; Satała, G.; Marciniak, K.; Pasierb, A.; Jastrzębska-Więsek, M.; Pawłowski, M.; Wesołowska, A.; Bojarski, A.J.; et al. The Impact of The Halogen Bonding on D(2) and 5-HT(1A)/5-HT(7) Receptor Activity of Azinesulfonamides of 4-[(2-ethyl)piperidinyl-1-yl]phenylpiperazines With Antipsychotic and Antidepressant Properties. *Bioorg. Med. Chem.* **2017**, *25*, 3638–3648. [\[CrossRef\]](#) [\[PubMed\]](#)
23. Kurczab, R.; Canale, V.; Satała, G.; Zajdel, P.; Bojarski, A.J. Amino Acid Hot Spots of Halogen Bonding: A Combined Theoretical and Experimental Case Study of the 5-HT(7) Receptor. *J. Med. Chem.* **2018**, *61*, 8717–8733. [\[CrossRef\]](#) [\[PubMed\]](#)
24. Zajdel, P.; Kos, T.; Marciniak, K.; Satała, G.; Canale, V.; Kamiński, K.; Hołuj, M.; Lenda, T.; Koralewski, R.; Bednarski, M.; et al. Novel Multi-Target Azinesulfonamides of Cyclic Amine Derivatives as Potential Antipsychotics with Pro-Social and Pro-Cognitive Effects. *Eur. J. Med. Chem.* **2018**, *145*, 790–804. [\[CrossRef\]](#)

25. Cheng, Y.; Prusoff, W.H. Relationship Between the Inhibition Constant (K<sub>1</sub>) and the Concentration of Inhibitor Which Causes 50 Per Cent Inhibition (I<sub>50</sub>) of an Enzymatic Reaction. *Biochem. Pharmacol.* **1973**, *22*, 3099–3108. [\[CrossRef\]](#)
26. Jiang, L.I.; Collins, J.; Davis, R.; Lin, K.-M.; DeCamp, D.; Roach, T.; Hsueh, R.; Rebres, R.A.; Ross, E.M.; Taussig, R.; et al. Use of a cAMP BRET Sensor to Characterize a Novel Regulation of cAMP by the Sphingosine 1-Phosphate/G<sub>13</sub> Pathway. *J. Biol. Chem.* **2007**, *282*, 10576–10584. [\[CrossRef\]](#)
27. Singh, J.K.; Solanki, A.; Shirsath, V.S. Comparative in-vitro Intrinsic Clearance of Imipramine in Multiple Species Liver Microsomes: Human, Rat, Mouse and Dog. *J. Drug Metab. Toxicol.* **2012**, *3*, 1–6. [\[CrossRef\]](#)
28. Canale, V.; Kotańska, M.; Dziubina, A.; Stefaniak, M.; Siwek, A.; Starowicz, G.; Marciniak, K.; Kasza, P.; Satała, G.; Duszyńska, B.; et al. Design, Sustainable Synthesis and Biological Evaluation of a Novel Dual  $\alpha_{2A}$ /5-HT<sub>7</sub> Receptor Antagonist with Antidepressant-Like Properties. *Molecules* **2021**, *26*, 3228. [\[CrossRef\]](#)
29. Koczurkiewicz-Adamczyk, P.; Gasiorkiewicz, B.; Piska, K.; Gunia-Krzyżak, A.; Jamrozik, M.; Bucki, A.; Słoczyńska, K.; Bojdo, P.; Wójcik-Pszczółka, K.; Władyka, B.; et al. Cinnamamide Derivatives With 4-Hydroxypiperidine Moiety Enhance Effect of Doxorubicin to Cancer Cells and Protect Cardiomyocytes Against Drug-Induced Toxicity Through CBR1 Inhibition Mechanism. *Life Sci.* **2022**, *305*, 120777. [\[CrossRef\]](#)
30. Colacino, E.; Porcheddu, A.; Charnay, C.; Delogu, F. From Enabling Technologies to Medicinal Mechanochemistry: An Eco-Friendly Access to Hydantoin-Based Active Pharmaceutical Ingredients. *React. Chem. Eng.* **2019**, *4*, 1179–1188. [\[CrossRef\]](#)
31. Canale, V.; Frisi, V.; Bantreil, X.; Lamaty, F.; Zajdel, P. Sustainable Synthesis of a Potent and Selective 5-HT(7) Receptor Antagonist Using a Mechanochemical Approach. *J. Org. Chem.* **2020**, *85*, 10958–10965. [\[CrossRef\]](#)
32. Bento, O.; Luttringer, F.; Mohy El Dine, T.; Pétry, N.; Bantreil, X.; Lamaty, F. Sustainable Mechanochemistry of Biologically Active Molecules. *European J. Org. Chem.* **2022**, e202101516. [\[CrossRef\]](#)
33. Andersen, J.; Brunemann, J.; Mack, J. Exploring Stable, Sub-ambient Temperatures in Mechanochemistry Via a Diverse Set of Enantioselective Reactions. *React. Chem. Eng.* **2019**, *4*, 1229–1236. [\[CrossRef\]](#)
34. Cindro, N.; Tireli, M.; Karadeniz, B.; Mrla, T.; Užarević, K. Investigations of Thermally Controlled Mechanochemical Milling Reactions. *ACS Sustain. Chem. Eng.* **2019**, *7*, 16301–16309. [\[CrossRef\]](#)
35. Kubota, K.; Baba, E.; Seo, T.; Ishiyama, T.; Ito, H. Palladium-Catalyzed Solid-State Borylation of Aryl Halides Using Mechanochemistry. *Beilstein J. Org. Chem.* **2022**, *18*, 855–862. [\[CrossRef\]](#)
36. Reynes, J.F.; Garcia, F. Temperature-Controlled Mechanochemistry Unlocks The Nickel-Catalyzed Suzuki-Miyaura-Type Coupling of Aryl Sulfamates at Different Scales. *Angew. Chemie Int. Ed.* **2022**. [\[CrossRef\]](#)
37. Chaumont-Dubel, S.; Dupuy, V.; Bockaert, J.; Bécamel, C.; Marin, P. The 5-HT(6) Receptor Interactome: New Insight in Receptor Signaling and Its Impact on Brain Physiology and Pathologies. *Neuropharmacology* **2020**, *172*, 107839. [\[CrossRef\]](#)
38. Allen, N.J.; Lyons, D.A. Glia as Architects of Central Nervous System Formation and Function. *Science* **2018**, *362*, 181–185. [\[CrossRef\]](#)
39. Giovannoni, F.; Quintana, F.J. The Role of Astrocytes in CNS Inflammation. *Trends Immunol.* **2020**, *41*, 805–819. [\[CrossRef\]](#)
40. Grychowska, K.; Chaumont-Dubel, S.; Kurczab, R.; Koczurkiewicz, P.; Deville, C.; Krawczyk, M.; Pietruś, W.; Satała, G.; Buda, S.; Piska, K.; et al. Dual 5-HT(6) and D(3) Receptor Antagonists in a Group of 1H-Pyrrolo[3,2-c]quinolines with Neuroprotective and Procognitive Activity. *ACS Chem. Neurosci.* **2019**, *10*, 3183–3196. [\[CrossRef\]](#)

**Disclaimer/Publisher's Note:** The statements, opinions and data contained in all publications are solely those of the individual author(s) and contributor(s) and not of MDPI and/or the editor(s). MDPI and/or the editor(s) disclaim responsibility for any injury to people or property resulting from any ideas, methods, instructions or products referred to in the content.